Research Article

For reprint orders, please contact: reprints@futuremedicine.com

Nanomedicine

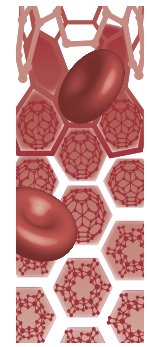

Comparison of nanoparticle penetration into solid tumors and sites of inflammation: studies using targeted and nontargeted liposomes

Aim: The vast majority of nanomedicine research is focused on the use of nanoparticles for the diagnosis and treatment of cancer. However, the dense extracellular matrix of solid tumors restricts nanoparticle penetration, raising the question of whether the best applications of nanomedicines lie in oncology. **Materials & methods:** In this study, the uptake of folate-conjugated liposomes was compared between folate receptor-expressing tumors and folate receptor+ inflammatory lesions within the same mouse. **Results:** We demonstrate here that both folate-targeted and nontargeted liposomes accumulate more readily at sites of inflammation than in solid tumors. **Conclusion:** These data suggest that nanosized imaging and therapeutic agents may be better suited for the treatment and diagnosis of inflammatory/autoimmune diseases than cancer.

Keywords: cancer • folate • inflammation • liposome • nanomedicine • nanoparticle

Scott Poh[1,2], Venkatesh Chelvam[1,3] & Philip S Low*[,1]

[1]Department of Chemistry, Purdue University, West Lafayette, IN 47907, USA

[2]Department of Biomedical Engineering, Purdue University, West Lafayette, IN 47907, USA

[3]Department of Chemistry, Indian Institute of Technology Indore, Madhya Pradesh, Indore 452017, India

*Author for correspondence: plow@purdue.edu

Use of nanoparticles (NPs) for medical applications has attracted considerable attention in recent years because of their enhanced drug loading capacities, ease of multifunctionalization, abilities to protect entrapped cargoes from physiological hazards, adaptability to passive and active targeting, and improved biocompatibility [1–6]. Not surprisingly, ten nanomedicines have achieved US FDA approval and an additional 29 are currently undergoing human clinical trials [6]. With the exception of five iron oxide formulations for MRI, all of the above NP formulations are designed for treatment of cancer [6,7].

While the application of nanomedicines to cancer therapy can obviously boast success, more detailed scrutiny of the formulations has revealed that their large sizes may compromise their abilities to penetrate deep into a tumor mass [5,8–9]. Thus, Torchilin and Jain disclosed in 1995 that tumor permeability was inversely proportional to NP radius [10]. Jain *et al.* (2001) then observed that permeation of NPs through solid tumors was further compromised by physical obstacles in the extracellular matrix that forced the NPs to follow more tortuous paths [11]. Publications by Grill *et al.* in 2002 and Kostarelos *et al.* in 2004 further revealed that liposomes primarily concentrate near the tumor vasculature, and fail to diffuse deeper into tumor masses [12–14]. Finally, in 2006, Dreher *et al* [15]. expanded on these analyses to explore the permeation of dextrans of molecular weights ranging from 3.3 to 2000 kDa into solid tumors. They reported that tumor penetration of 40–70 kDa dextrans was largely limited to 15 μm from the nearest capillary and penetration of 2000 kDa dextrans was mainly restricted to only approximately 5 μm from the closest vessel wall. Taken together, these data raise the question whether cancer therapy constitutes the best indication for NPs in medicine.

In this paper, we compare the abilities of folate-targeted liposomes to deliver their cargos into tumors and inflamed lesions within the same animal (Figure 1). The folate receptor (FR) is a 38-kDa glycosylphosphatidylinositol anchored protein

Future Medicine part of fsg

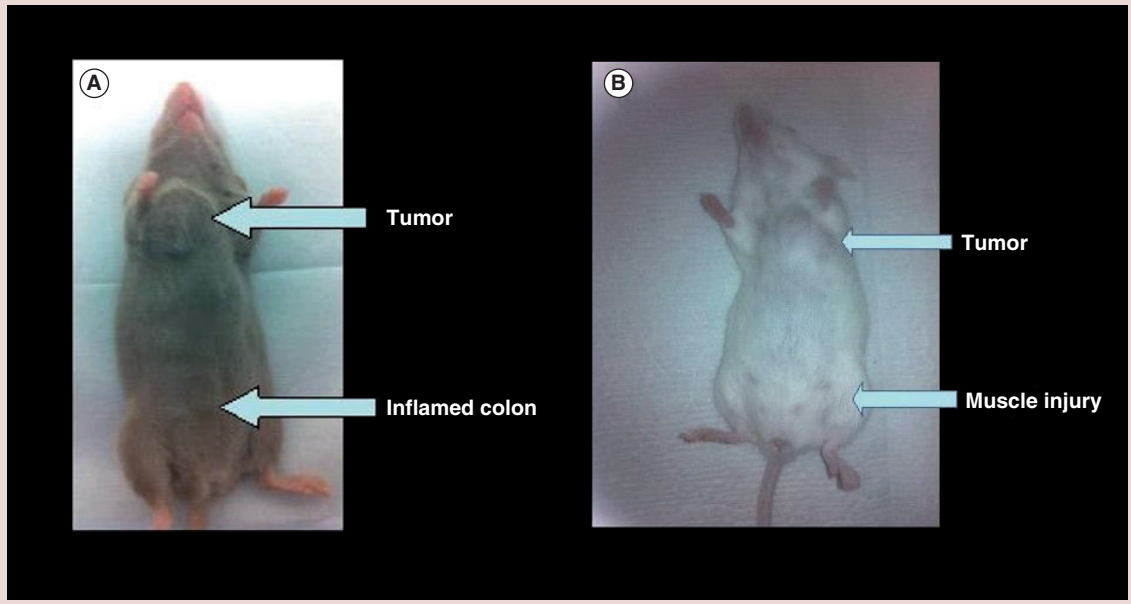

Figure 1. Mouse model of inflammation and tumors. (A) Tumor and inflamed colon, and **(B)** tumor and muscle injury.

that binds the vitamin folic acid with high affinity (~1 nM). Conjugation of folic acid to small molecules, proteins, and liposomes permits their binding and internalization into FR+ cells by receptor-mediated endocytosis [2,16–18]. Because many cancer cell types overexpress FRs, it is possible to selectively target folate-derivatized cargoes to malignant cells within FR+ tumors [3,9,18–19]. Similarly, because activated macrophages (but not resting macrophages or other hematopoietic cells) also overexpress FRs, folate-linked liposomes can also be targeted to sites of inflammation that characterize many autoimmune diseases [17,20]. Moreover, our previously reported studies aimed at imaging sites of inflammation with either NPs or small molecule imaging agents in both humans and animal models clearly demonstrate that the vast majority of activated macrophages remain stationary at the inflamed loci, since uptake at these sites (and not elsewhere in the body) is invariably observed [21–23]. Because it is possible to grow FR+ tumors in mice that are also induced to develop FR+ inflammatory/autoimmune lesions, a direct comparison of the ability of folate-derivatized liposomes to target tumors versus inflamed tissues can be obtained. We report below that folate-conjugated liposomes preferentially accumulate in inflamed tissues when present in mice containing FR+ tumors, regardless of the tumor type or inflammatory disease examined. These data suggest that the overwhelming emphasis on use of nanomedicines in oncology may need to be reconsidered.

Materials & methods

Preparation of liposomes

Lipids and cholesterol were purchased from Avanti Polar Lipids (AL, USA) and used without further purification. Folate-PEG_{3400}-DSPE (1,2-distearoyl-*sn*-glycero-3-phosphoethanolamine-*N*-[folate (polyethylene glycol)-3400]) (1) was synthesized according to a previously reported procedure [2–3,24]. Folate-targeted and nontargeted liposomes were composed of the following:

Folate-PEG-liposomes (Fol-liposomes) were formulated with DSPC (distearoyl-*sn*-glycero-3-phosphocholine)/cholesterol/PEG_{2000}-DSPE (1,2-distearoyl-*sn*-glycero-3-phosphoethanolamine-*N*-[methoxy(polyethyleneglycol)-2000])/folate-PEG_{3400}-DSPE (1) in the ratio 56:40:4:0.1;

Nontargeted liposomes (NT-liposome) were formulated using DSPC/cholesterol/PEG_{2000}-DSPE in the ratio 56:40:4.

Fluorescent liposomes (liposome-DiD) loaded with DiD (1,1′-dioctadecyl-3,3,3′,3′-tetramethylindodicarbocyanine) were prepared by polycarbonate membrane extrusion [3,18]. Lipid mixtures were dissolved in $CHCl_3$ and dried on a rotary evaporator at 55°C and then under vacuum to complete dryness. The lipid film was then hydrated with 1% DiD in phosphate-buffered saline (PBS; 20 mM Na_2HPO_4, 120 mM NaCl, pH 7.4) buffer. Rehydration was accomplished by vigorous vortexing followed by ten cycles of freezing and thawing. The lipid suspension was then extruded ten-times each through 400, 200 and 100 nm polycarbonate mem-

branes using a 10 ml thermobarrel extruder (Lipex Biomembranes, BC, Canada) driven by a positive pressure of Argon. The liposomes were purified by size exclusion chromatography on a Sepharose CL-4B column equilibrated in PBS to produce a suspension of unilamellar liposomes. The stability of these liposomes have been reported previously [25].

Radiolabeled liposomes were formulated using a modification of the above procedure[4]. Briefly, a 56:40:4 molar ratio of DSPC:CHOL:DSPE-PEG was dissolved in EtOH/$CHCl_3$ (50°C) containing 250 µCi [^{3}H] cholesterol hexadecyl ester. [^{3}H] Liposomes were then prepared by thin lipid film hydration followed by extrusion ten-times through a 0.2 µm filter and then ten-times through a 0.1 µm filter using a 10 ml Lipex Thermoline extruder (Northern Lipids, BC, Canada) at 60°C. The liposomes were purified by size exclusion chromatography on a Sepharose CL-4B column equilibrated in PBS to produce a suspension of unilamellar liposomes.

Size distribution of liposomes

Liposomes used in these studies all ranged from 100 to 110 nm in diameter.

Cell culture & animal husbandry

L1210A and M109 cells were grown continuously as a monolayer in folate-free RPMI medium containing 10% fetal calf serum and a 1% penicillin and streptomycin antibiotic cocktail in 5% CO_2:95% air-humidified atmosphere at 37°C.

All animal procedures were approved by the Purdue Animal Care and Use Committee (PACUC) in accordance with guidelines of the National Institute of Health. All animals were maintained on a folate-deficient diet (Teklad; Harlan Laboratories Inc.) for at least 3 weeks prior to each study in order to reduce serum folate levels to physiological levels. Control animals were also maintained on a folate-deficient diet [26].

Subcutaneous tumor generation & induction of either ulcerative colitis or muscle injury in mice

Six-week-old male DBA/2 or Balb/c mice (Harlan Laboratories, IN, USA) maintained on a folate deficient diet were inoculated subcutaneously on the ventral thorax with FR+ M109 or L1210A cancer cells (1.0×10^6 cells/mouse in RPMI medium), using a pre-

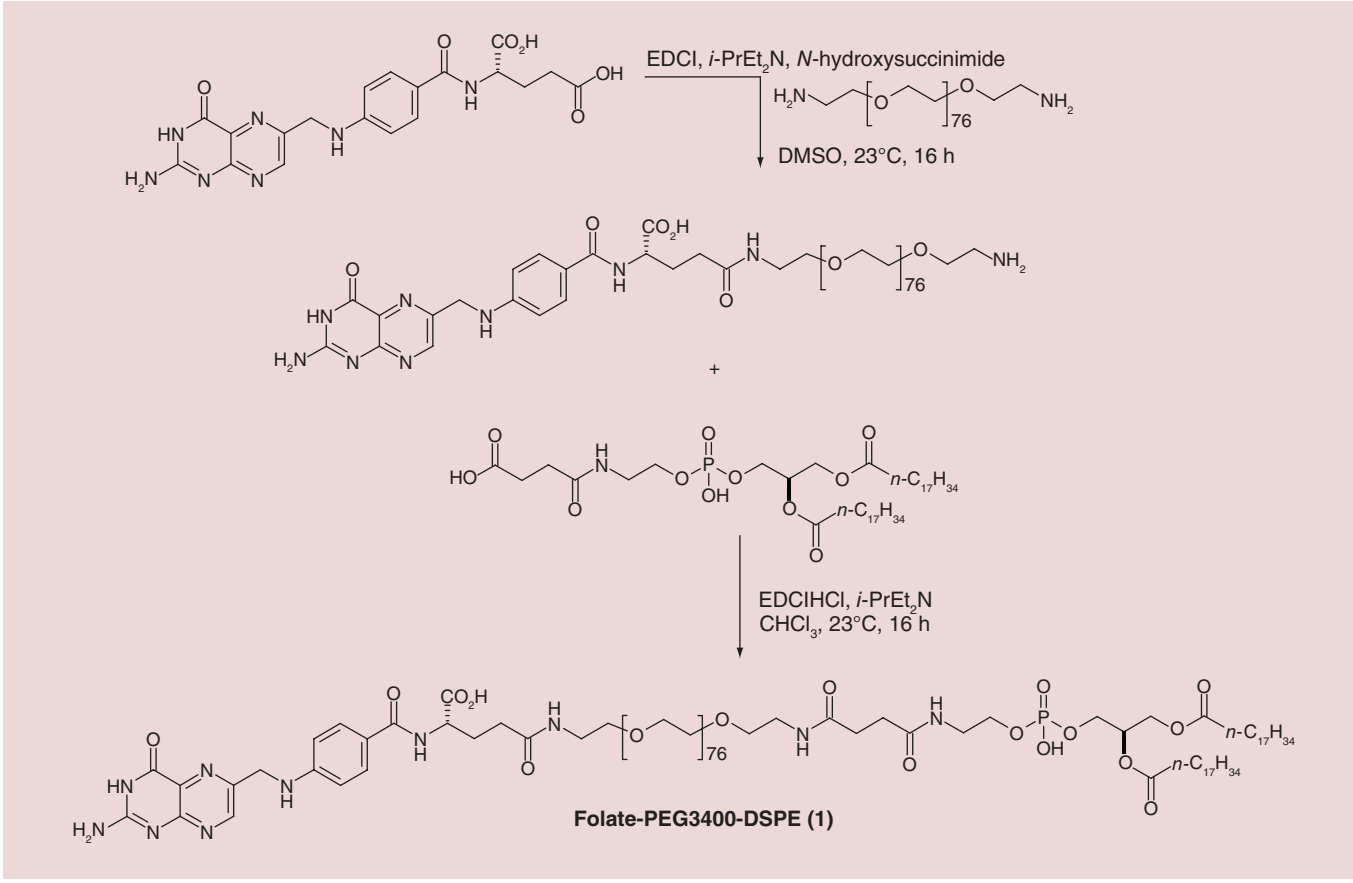

Figure 2. Synthesis of folate-PEG3400-DSPE liposome targeting ligand 1.
DMSO: Dimethylsulfoxide; DSPE: 1,2-diastearoyl-glycero-3-phosphoethanolamine.

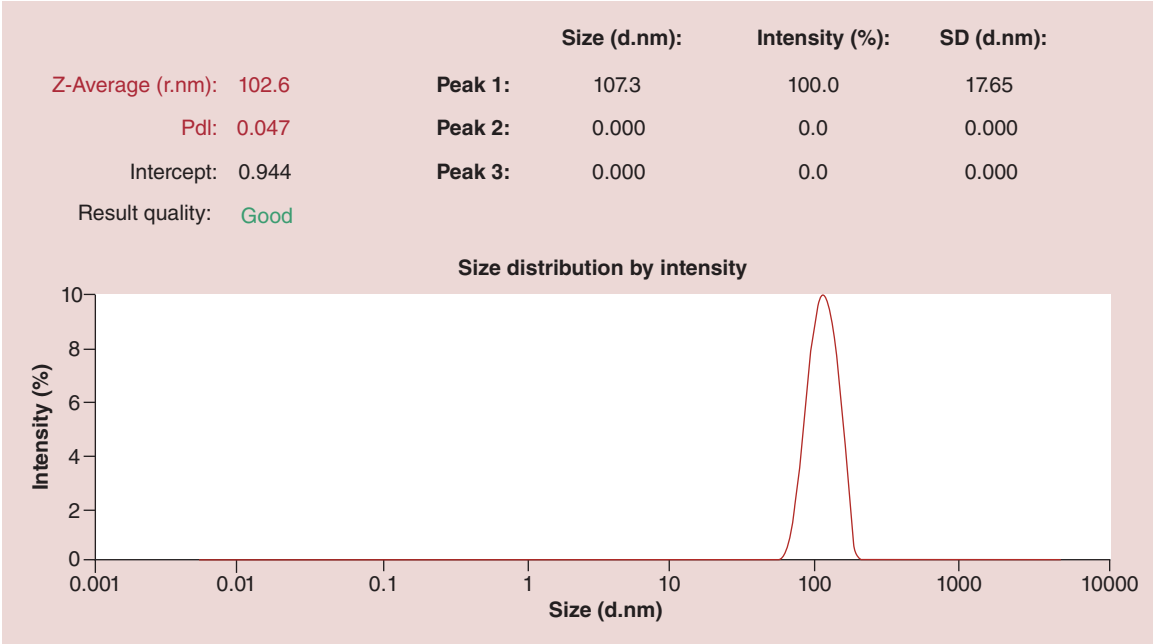

Figure 3. Representative dynamic light scattering of nontargeted liposomes.
d.nm: Diameter (nm); PdI: Polydispersity index; SD: Standard deviation.

viously reported procedure [26]. Subcutaneous tumor growth was monitored daily and on day 11 post-tumor inoculation, 3% dextran sodium sulfate (DSS) was added to their drinking water for a period of 6 days to induce ulcerative colitis (UC). The animals were then randomly divided into different groups and injected into the tail vein with the desired liposome preparation. The animals were sacrificed 10 h after injection of liposomes by CO_2 asphyxiation, and images were acquired as described below.

For the model of muscle injury, tumor-bearing mice were injected with snake venom cardiotoxin from the Chinese cobra (*Naja atra*) on day 12 post-tumor inoculation [27]. Briefly, the mice were anaesthetized with 3% isoflurane, and the tibialis anterior (TA) muscle of each mouse was injected with 100 µl of cardiotoxin I (Sigma-Aldrich). Four days after cardiotoxin injection, the tumor-bearing rodents were injected intravenously with folate-targeted liposomes loaded with DiD (Fol-liposomes-DiD) or nontargeted liposomes loaded with DiD (NT-liposome-DiD). The animals were sacrificed 12 h after injection by CO_2 asphyxiation, and images were recorded as described below.

In vivo fluorescence imaging of mice

Imaging of mice was performed using a Kodak Imaging Station connected to a charge-coupled device camera operated with Kodak Molecular Imaging Software (version 4.0; Carestream Molecular Imaging). For white light imaging, the following camera parameters were used: acquisition time 0.05 s, f-stop 11, focal plane 7, field of view 200 and no binning. For fluorescence imaging, the following parameters were used: acquisition time 30 s, excitation filter of λ = 625 nm, emission filter of λ = 700 nm, f-stop 4, focal plane 7, field of view 200 and binning 4 [26].

^{3}H-liposome biodistribution study

Twenty days after tumor cell inoculation (described above) each mouse received 1 mg of liposomes containing 250 µCi cholesterol hexadecyl ester (PerkinElmer, MA, USA). Animals were euthanized 48 h later, and their tissues harvested. Solid tumors and inflamed tissues were excised. Individual tissue samples were digested with Soluene 350® (PerkinElmer), bleached to uniform color using hydrogen peroxide, then added to Hionic-Fluor® scintillation cocktail (PerkinElmer) for counting using a liquid scintillation counter (Packard BioScience, CT, USA) [18]. The accumulated radioactivity in each sample is expressed as a percentage of the injected dose per gram of wet tissue (%ID/g). A student's unpaired t-test was used for all comparisons, with $p < 0.05$ considered statistically significant. Competition studies were also performed to confirm that folate-targeted liposome uptake by tumors and sites of inflammation was mediated by FRs [18].

Results & discussion

For this study, liposomes composed of 1,2-diastearoyl-glycero-3-phosphoethanolamine (DSPE) and distearoyl-*sn*-glycero-3-phosphocholine (DSPC) of

approximately 100 nm diameter were prepared. Targeted liposomes were formulated by addition of 0.1% folate-conjugated DSPE 1. The synthesis of 1 is outlined in Figure 2, and the properties of the resulting folate-targeted liposomes have been described previously [2,3,18,25].

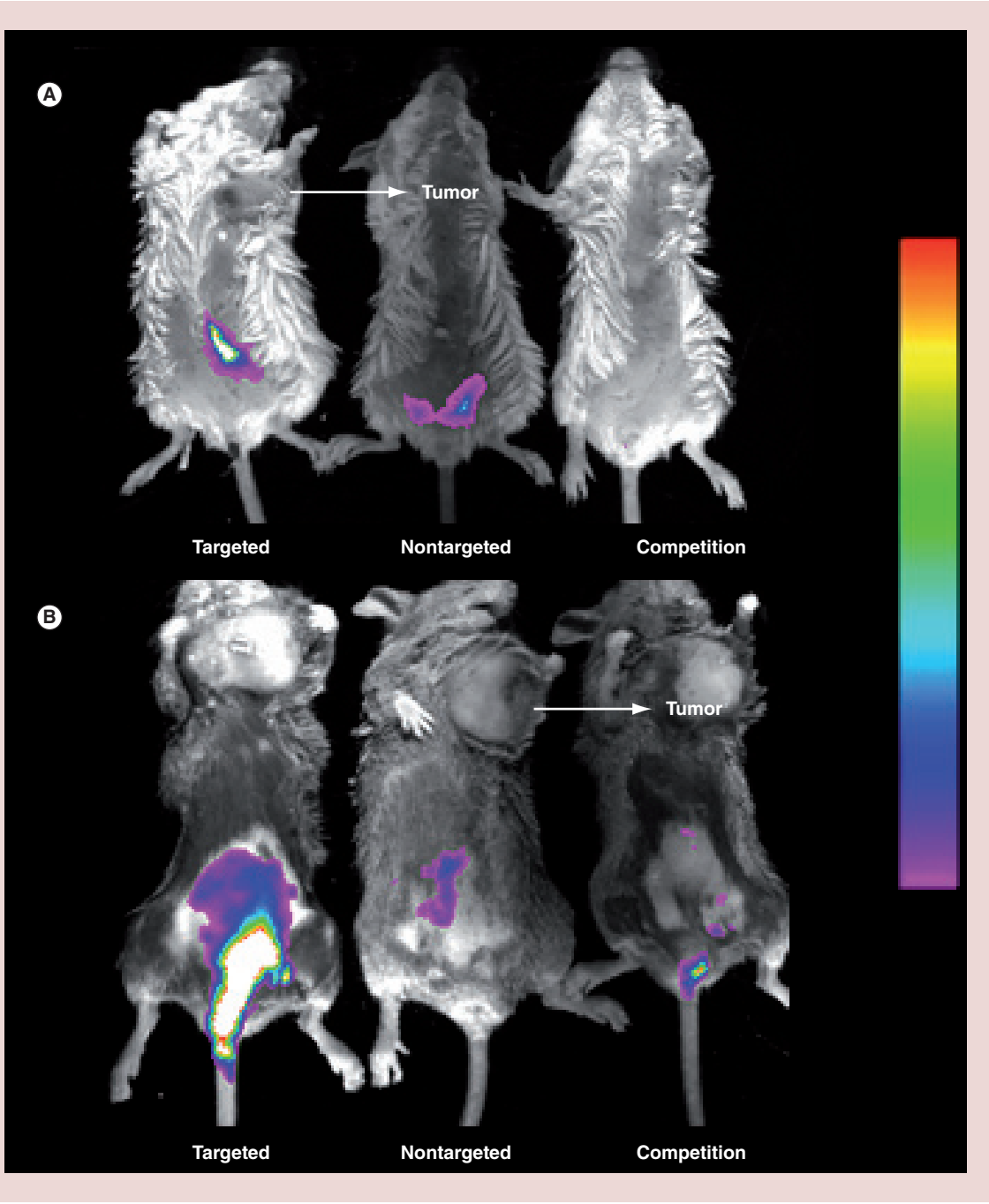

Figure 4. Imaging of folate-targeted liposome uptake in mice induced to develop ulcerative colitis and implanted with folate receptor-positive tumors. Uptake of fluorescent liposomes in Balb/C mice with ulcerative colitis and M109 tumors **(A)**, or DBA/2 mice with ulcerative colitis and L1210A tumors **(B)** was imaged using a Kodak Imaging Station. Mice were injected (tail vein) with folate-targeted liposomes loaded with DiD (targeted), NT-liposome-DiD (nontargeted), or a 100-fold excess of unlabeled folate-PEG-liposomes to block all available folate receptors, followed by folate-targeted liposomes loaded with DiD 1 h later (competition). Images were obtained 12 h after liposome injection.
DiD: 1,1′-dioctadecyl-3,3,3′,3′-tetramethylindodicarbocyanine.

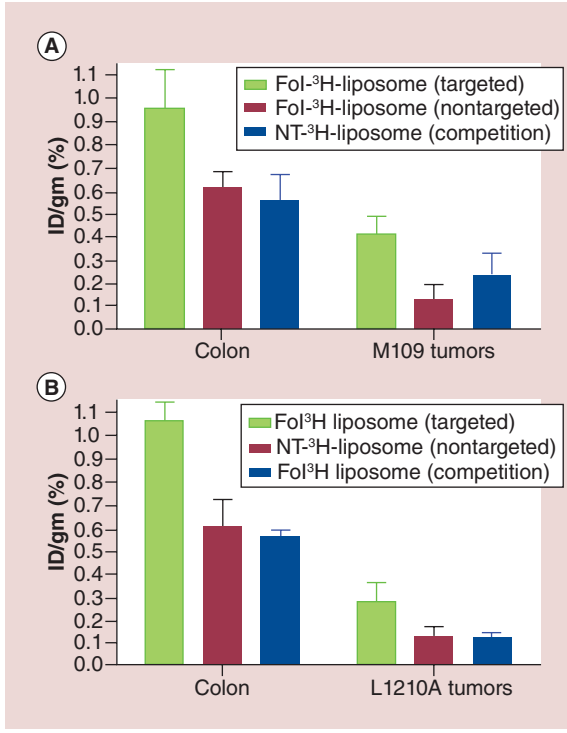

Figure 5. Biodistribution of liposomes in mice induced with ulcerative colitis and implanted with subcutaneous syngeneic tumors. Balb/C mice with ulcerative colitis and M109 tumors **(A)**, or DBA/2 mice with ulcerative colitis and L1210A tumors **(B)** were injected (tail vein) with Fol-^{3}H-liposome (targeted), or NT-^{3}H-liposome (nontargeted), a 100-fold excess of Fol-liposomes to block all available folate receptors, followed 1 h later by Fol-^{3}H-liposome (competition), with n = 5 mice/group. Mice were euthanized, resected, and tissues were counted 48 h after liposome injection. Fol: Folate; ID: Injected dose per gram (%); NT: Nontargeted.

Fluorescent liposomes were prepared by encapsulating 1,1′-dioctadecyl-3,3,3′,3′-tetramethylindodicarbocyanine (DiD).

DiD was selected because of its emission at relatively long wavelength (~ 700 nm), which allows for better visualization deep within tissues [20]. Fol-liposomes-DiD, nontargeted fluorescent liposomes (NT-liposome-DiD), and folate-targeted nonfluorescent liposomes (Fol-liposomes) were then used in experiments described below.

Comparison of liposome accumulation in inflamed tissues relative to solid tumors required induction of both pathologies in the same animal. Syngeneic tumor models examined included Balb/C mice implanted subcutaneously with M109 lung cancer cells and DBA/2 mice implanted with L1210A lymphocytic leukemia cells. UC was initiated by inclusion of dextran sodium sulfate (DSS) in the drinking water. Following tail vein injection of the desired liposome formulation, uptake of the labeled liposomes was imaged using a Kodak Imaging Station. As shown in Figure 3, neither of the fluorescent liposomes exhibited prominent uptake in either of the implanted tumors, while both accumulated readily in the inflamed colons (see both Figure 3A & B). Moreover, Fol-liposomes-DiD exhibited greater uptake than its nontargeted counterpart in the ulcerated colons, suggesting that Fol-liposomes-DiD is internalized more readily than the nontargeted liposomes. The modest uptake of NT-liposome-DiD in the colons was likely due to nonspecific phagocytosis by immune cells.

In order to demonstrate that Fol-liposomes-DiD uptake was FR-mediated, a competition experiment was performed, where an excess of Fol-liposomes containing no fluorescent dye was injected into the mice and allowed to saturate all available FRs. Fol-liposomes-DiD were then injected, and fluorescence images were again taken. As shown in the mice on the right, little or no fluorescence was detected, confirming that uptake of Fol-liposomes-DiD is FR mediated.

To demonstrate that these results are not unique to inflamed tissues associated with ulcerative colitis, we investigated the relative uptake of the same liposome formulations in a second model of inflammation in tumor-bearing mice containing the same tumors. Snake venom cardiotoxin from the Chinese cobra (*Naja atra*) was injected into a hind limb of the mice to induce muscle trauma and the associated inflammation [27]. Then, after injection of Fol-liposomes-DiD, NT-liposome-DiD, or Fol-liposomes-DiD competed with excess unlabeled Fol-liposomes mice were again imaged as described above. As seen in Figure 4, accumulation in the injured muscle tissue was significant for the targeted liposomes, but less prominent for both nontargeted and competed liposomes. Moreover, uptake in the tumor tissue, regardless of whether a lung cancer (M109) or lymphoma (L1210A) model was employed, was negligible. And as seen before, competition with excess unlabeled FR-targeted liposomes prevented capture of the targeted liposomes, demonstrating that the accumulation of folate-targeted liposomes in the inflamed tissues was FR mediated.

In order to quantitatively evaluate the difference in accumulation at sites of inflammation versus tumors, a biodistribution study was carried out in the same mouse models using either folate-targeted or nontargeted liposomes containing ^{3}H-cholesteryl hexadecyl ester. The accumulated radioactivity (expressed as% injected dose per gram of excised wet tissue (ID/gm [%]) in each tissue was then measured and compared [18].

For this purpose, mice implanted with subcutaneous M109 or L1210A tumors and induced to develop ulcerative colitis were injected with either Fol-^{3}H-liposomes or NT-^{3}H-liposomes. As seen in Figure 5 uptake

of the folate-targeted liposomes was twofold to fourfold higher in the inflamed colons than in the tumors. Modest accumulation of nontargeted NT-^{3}H-liposomes occurred in both colons and tumors (perhaps

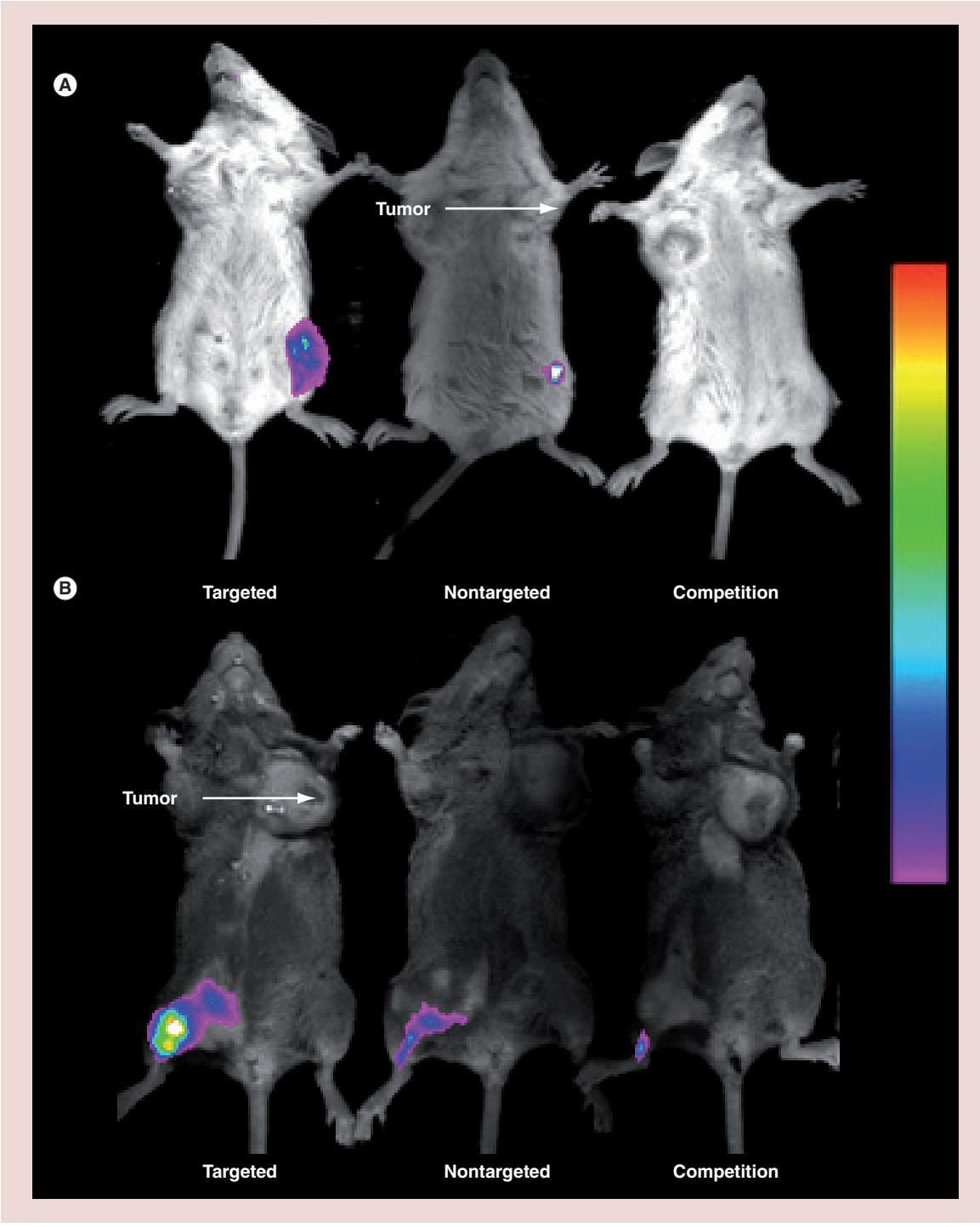

Figure 6. Imaging of mice with trauma-induced muscle inflammation and subcutaneous solid tumors. Balb/C mice with muscle trauma and M109 tumors **(A)**, or DBA/2 mice with muscle trauma and L1210A tumors **(B)** were injected (tail vein) with the following: folate-targeted liposomes loaded with DiD (targeted), NT-liposome-DiD (nontargeted), a 100-fold excess of folate-PEG-liposomes to block all available folate receptors, followed by folate-targeted liposomes loaded with DiD 1 h later (competition). Images were obtained 10 h after liposome injection. Arrows indicate the locations of tumor masses.
DiD: 1,1′-dioctadecyl-3,3,3′,3′-tetramethylindodicarbocyanine.

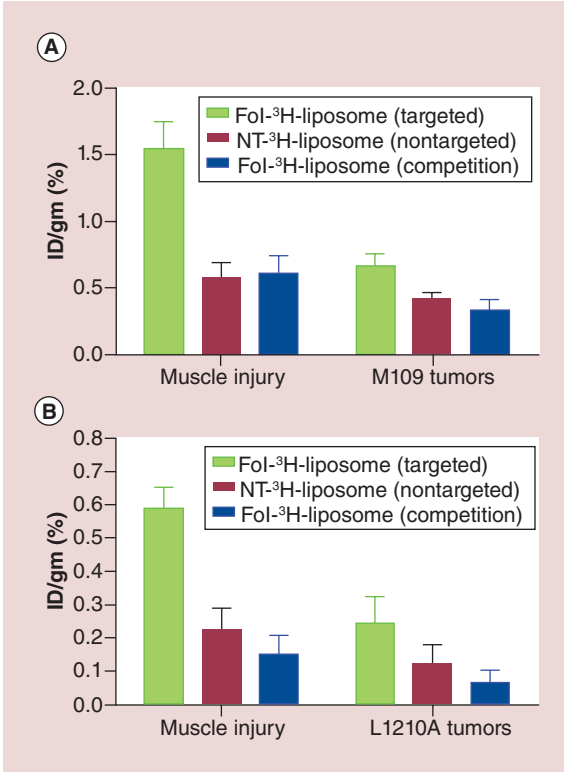

Figure 7. Biodistribution of liposomes in mice with trauma induced muscle inflammation and implanted with subcutaneous syngeneic tumors. Balb/C mice with ulcerative colitis and M109 tumors **(A)**, or DBA/2 mice with ulcerative colitis and L1210A tumors **(B)** were injected (tail vein) with Fol-^{3}H-liposome (targeted), or NT-^{3}H-liposome (nontargeted), a 100-fold excess of Fol-liposomes to block all available folate receptors, followed 1 h later by Fol-^{3}H-liposome (competition), with n = 5 mice/group. Mice were euthanized, resected, and tissues were counted 48 h after liposome injection. Fol: Folate; ID: Injected dose per gram (%); NT: Nontargeted.

due to phagocytosis by macrophages or EPR-mediated passive uptake in the tumors); however, folate targeting enhanced uptake in all tissues, with twofold to 3.5-fold higher accumulation observed for Fol-^{3}H-liposome than NT-^{3}H-liposomes (Figure 5).

A competition experiment was also performed to confirm that uptake of Fol-^{3}H-liposome was FR-mediated. As seen in Figure 5, blockade of unoccupied FRs with excess unlabeled Fol-liposomes yielded colon and tumor uptake values similar to nontargeted liposomes, demonstrating that nonspecific uptake in both the tumors and inflamed tissue does occur, but that folate-targeting is able to significantly increase accumulation at these sites.

A second biodistribution study was then performed to confirm these results using the muscle injury instead of the UC model of inflammation. In this case, uptake in the inflamed tissues of the mice was approximately double that of either M109 or L1210A tumor (Figure 6). Folate-targeting of the ^{3}H-liposomes again improved uptake, with a 2.8-fold increase in liposome retention in inflamed muscle, and a 1.5 to twofold greater accumulation in the tumors.

Conclusion

Because many cancers overexpress a folate receptor (FR-α) and virtually all inflamed lesions accumulate FR-β positive macrophages [28–31], it was possible to compare the relative uptake of both ligand-targeted and nontargeted NPs (liposomes) by malignant versus inflamed lesions in the same animal. Our data from multiple animal models now demonstrate that NP uptake by FR+ inflamed tissues always exceeds NP uptake by FR+ malignant tissues, regardless of whether the liposomes are targeted or not. For the targeted liposomes, uptake in inflamed lesions exceeded accumulation in the tumor masses by a factor of 2.3–3.8-fold, depending of the tumor type and nature of inflammatory disease examined. While these differences are compelling in their own right, the differences probably constitute a vast underestimate, since the tumor mass is comprised primarily of cancer cells whereas the inflamed lesions consist predominantly of the normal tissue, with activated macrophages contributing only a small fraction of the total cell population. Moreover, the cancer cell lines that we employed both express >10^6 FRs/cell [32–35], whereas the average activated macrophage expresses between 100,000 and 200,000 FRs/cell. Thus, the opportunity for a folate-derivatized liposome to encounter an FR-expressing cell is much greater in the tumor mass than in the inflamed lesions. The fact that the liposomes still accumulated more intensely at the sites of inflammation argues strongly for more pervasive penetration of the NPs into the inflamed than malignant tissues.

Although only two models of inflammation were examined in this study, the general conclusions should still be relevant for virtually all inflammatory and autoimmune diseases. Thus, folate receptor positive macrophages have been shown to accumulate in inflamed lesions of patients with rheumatoid arthritis, Crohn's disease, atherosclerosis, osteoarthritis, Sjogren's syndrome, ischemia reperfusion injury, vasculitis, idiopathic pulmonary fibrosis, asthma, psoriasis and multiple sclerosis [31,36–42], and these same sites of inflammation are characterized by increased vascular permeability due to the prominent release of such regulators of endothelial function as TNF-α [43], VEGF [44], histamine [45] and IL-2 [46]. By contrast, while solid tumors are often characterized by a leaky vasculature, their dense extracellular matrices and high cellular densities can strongly suppress NP permeation

beyond the capillary wall. Because targeted NPs can only dock onto their cognate receptors if they can reach the targeted cell surface, uptake of both targeted and nontargeted NPs may be determined more by their ease of passage between tumor cells than by their abilities to exit the vasculature. The fact that tumor accumulation of our FR-targeted liposomes exceeded accumulation of the nontargeted liposomes by only twofold to threefold (Figures 4 & Figure 7, while delivery of FR-targeted small molecules exceeds that of nontargeted small molecules by approximately 50-fold [47], suggests that particle size rather than FRs availability determines the magnitude of NP uptake into solid tumors.

Future perspective

Interrogation of literature databases over the last 5 years reveals that a 100-times more nanomedicine publications have focused on oncology than autoimmunity and related pathologies [48]. Given the better accessibility of NPs to sites of inflammation established here, we envisage an increased exploration of NP formulations for treatment of autoimmune and inflammatory diseases, with special emphasis on biodegradable polymers where chronic administration is required [49]. We also anticipate that many current NP formulations that prove ineffective in oncology applications may still find utility in the autoimmune or inflammatory disease field.

Financial & competing interests disclosure

The authors have no relevant affiliations or financial involvement with any organization or entity with a financial interest in or financial conflict with the subject matter or materials discussed in the manuscript. This includes employment, consultancies, honoraria, stock ownership or options, expert testimony, grants or patents received or pending, or royalties.

No writing assistance was utilized in the production of this manuscript.

Ethical conduct of research

The authors state that they have obtained appropriate institutional review board approval or have followed the principles outlined in the Declaration of Helsinki for all human or animal experimental investigations. In addition, for investigations involving human subjects, informed consent has been obtained from the participants involved.

Executive summary

Background

- The overwhelming majority of nanomedicine research is focused on the use of nanoparticles for the diagnosis and treatment of cancer.
- Solid tumors often possess a dense extracellular matrix that restricts deep penetration throughout the tumor.

Results & discussion

- The uptake of folate-conjugated liposomes was compared between folate receptor-expressing tumors and folate receptor+ inflammatory lesions were studied within the same mouse.
- We demonstrate that both folate-targeted and nontargeted liposomes accumulate more readily at sites of inflammation than in solid tumors.
- Targeted nanoparticles were taken up more aggressively than their nontargeted counterparts.

Conclusion

- Nanosized imaging and therapeutic agents may be better suited for the treatment and diagnosis of inflammatory/autoimmune diseases than cancer.

References

1 Kawasaki ES, Player A. Nanotechnology, nanomedicine, and the development of new, effective therapies for cancer. *Nanomedicine* 1(2), 101–109 (2005).

2 Leamon CP, Cooper SR, Hardee GE. Folate-liposome-mediated antisense oligodeoxynucleotide targeting to cancer cells: evaluation *in vitro* and *in vivo*. *Bioconjug. Chem.* 14(4), 738–747 (2003).

3 Lee RJ, Low PS. Delivery of liposomes into cultured KB cells via folate receptor-mediated endocytosis. *J. Biol. Chem.* 269(5), 3198–3204 (1994).

4 Markman JL, Rekechenetskiy A, Holler E, Ljubimova JY. Nanomedicine therapeutic approaches to overcome cancer drug resistance. *Adv. Drug. Deliv. Rev.* 65(13–14), 1866–1879 (2013).

5 Waite CL, Roth CM. Nanoscale drug delivery systems for enhanced drug penetration into solid tumors: current progress and opportunities. *Crit. Rev. Biomed. Eng.* 40(1), 21–41 (2012).

6 Wang R, Billone PS, Mullett WM. Nanomedicine in action: an overview of cancer nanomedicine on the market and in clinical trials. *J. Nanomaterials* 2013, 12 (2013).

7 Xia W, Low PS. Folate-targeted therapies for cancer. *J. Med. Chem.* 53(19), 6811–6824 (2010).

8 Goodman TT, Olive PL, Pun SH. Increased nanoparticle penetration in collagenase-treated multicellular spheroids. *Int. J. Nanomedicine* 2(2), 265–274 (2007).

9 Choi IK, Strauss R, Richter M, Yun CO, Lieber A. Strategies to increase drug penetration in solid tumors. *Front. Oncol.* 3, 193 (2013).

10 Yuan F, Dellian M, Fukumura D *et al.* Vascular permeability in a human tumor xenograft: molecular size dependence and cutoff size. *Cancer Res.* 55(17), 3752–3756 (1995).

11 Pluen A, Boucher Y, Ramanujan S *et al.* Role of tumor-host interactions in interstitial diffusion of macromolecules: cranial vs. subcutaneous tumors. *Proc. Natl Acad. Sci. USA* 98(8), 4628–4633 (2001).

12 Grill J, Lamfers ML, Van Beusechem VW *et al.* The organotypic multicellular spheroid is a relevant three-dimensional model to study adenovirus replication and penetration in human tumors *in vitro*. *Mol. Ther.* 6(5), 609–614 (2002).

13 Emfietzoglou D, Kostarelos K, Papakostas A *et al.* Liposome-mediated radiotherapeutics within avascular tumor spheroids: comparative dosimetry study for various radionuclides, liposome systems, and a targeting antibody. *J. Nucl. Med.* 46(1), 89–97 (2005).

14 Kostarelos K, Emfietzoglou D, Papakostas A, Yang WH, Ballangrud A, Sgouros G. Binding and interstitial penetration of liposomes within avascular tumor spheroids. *Int. J. Cancer* 112(4), 713–721 (2004).

15 Dreher MR, Liu W, Michelich CR, Dewhirst MW, Yuan F, Chilkoti A. Tumor vascular permeability, accumulation, and penetration of macromolecular drug carriers. *J. Natl Cancer Inst.* 98(5), 335–344 (2006).

16 Cho K, Wang X, Nie S, Chen ZG, Shin DM. Therapeutic nanoparticles for drug delivery in cancer. *Clin. Cancer Res.* 14(5), 1310–1316 (2008).

17 Turk MJ, Reddy JA, Chmielewski JA, Low PS. Characterization of a novel pH-sensitive peptide that enhances drug release from folate-targeted liposomes at endosomal pHs. *Biochim. Biophys. Acta* 1559(1), 56–68 (2002).

18 Turk MJ, Waters DJ, Low PS. Folate-conjugated liposomes preferentially target macrophages associated with ovarian carcinoma. *Cancer Lett.* 213(2), 165–172 (2004).

19 Henne WA, Rothenbuhler R, Ayala-Lopez W, Xia W, Varghese B, Low PS. Imaging sites of infection using a 99mTc-labeled folate conjugate targeted to folate receptor positive macrophages. *Mol. Pharm.* 9(5), 1435–1440 (2012).

20 Yefimova SL, Kurilchenko IY, Tkacheva TN *et al.* Comparative study of dye-loaded liposome accumulation in sensitive and resistant human breast cancer cells. *Exp. Oncol.* 34(2), 101–106 (2012).

21 Paulos CM, Turk MJ, Breur GJ, Low PS. Folate receptor-mediated targeting of therapeutic and imaging agents to activated macrophages in rheumatoid arthritis. *Adv. Drug. Deliv. Rev.* 56(8), 1205–1217 (2004).

22 Turk MJ, Breur GJ, Widmer WR *et al.* Folate-targeted imaging of activated macrophages in rats with adjuvant-induced arthritis. *Arthritis Rheum.* 46(7), 1947–1955 (2002).

23 Xia W, Hilgenbrink AR, Matteson EL, Lockwood MB, Cheng JX, Low PS. A functional folate receptor is induced during macrophage activation and can be used to target drugs to activated macrophages. *Blood* 113(2), 438–446 (2009).

24 Lee RJ, Low PS. Folate-mediated tumor cell targeting of liposome-entrapped doxorubicin *in vitro*. *Biochim. Biophys. Acta* 1233(2), 134–144 (1995).

25 Lee RJ, Wang S, Turk MJ, Low PS. The effects of pH and intraliposomal buffer strength on the rate of liposome content release and intracellular drug delivery. *Biosci. Rep.* 18(2), 69–78 (1998).

26 Vaitilingam B, Chelvam V, Kularatne SA, Poh S, Ayala-Lopez W, Low PS. A folate receptor-alpha-specific ligand that targets cancer tissue and not sites of inflammation. *J. Nucl. Med.* 53(7), 1127–1134 (2012).

27 Vignaud A, Hourde C, Butler-Browne G, Ferry A. Differential recovery of neuromuscular function after nerve/muscle injury induced by crude venom from Notechis scutatus, cardiotoxin from Naja atra and bupivacaine treatments in mice. *Neurosci. Res.* 58(3), 317–323 (2007).

28 Varghese B, Vlashi E, Xia W *et al.* Folate receptor-beta in activated macrophages: ligand binding and receptor recycling kinetics. *Mol. Pharm.* 11(10), 3609–3616 (2014).

29 Zhao X, Li H, Lee RJ. Targeted drug delivery via folate receptors. *Expert Opin. Drug Deliv.* 5(3), 309–319 (2008).

30 Shen J, Hilgenbrink AR, Xia W *et al.* Folate receptor-beta constitutes a marker for human proinflammatory monocytes. *J. Leukoc. Biol.* 96(4), 563–570 (2014).

31 Thomas TP, Goonewardena SN, Majoros IJ *et al.* Folate-targeted nanoparticles show efficacy in the treatment of inflammatory arthritis. *Arthritis Rheum.* 63(9), 2671–2680 (2011).

32 Leamon CP, Reddy JA, Dorton R *et al.* Impact of high and low folate diets on tissue folate receptor levels and antitumor responses toward folate-drug conjugates. *J. Pharmacol. Exp. Ther.* 327(3), 918–925 (2008).

33 Lu Y, Xu LC, Parker N *et al.* Preclinical pharmacokinetics, tissue distribution, and antitumor activity of a folate-hapten conjugate-targeted immunotherapy in hapten-immunized mice. *Mol. Cancer Ther.* 5(12), 3258–3267 (2006).

34 Parker N, Turk MJ, Westrick E, Lewis JD, Low PS, Leamon CP. Folate receptor expression in carcinomas and normal tissues determined by a quantitative radioligand binding assay. *Anal. Biochem.* 338(2), 284–293 (2005).

35 Reddy JA, Xu LC, Parker N, Vetzel M, Leamon CP. Preclinical evaluation of (99m)Tc-EC20 for imaging folate receptor-positive tumors. *J. Nucl. Med.* 45(5), 857–866 (2004).

36 Henne WA, Kularatne SA, Ayala-Lopez W *et al.* Synthesis and activity of folate conjugated didemnin B for potential treatment of inflammatory diseases. *Bioorg. Med. Chem. Lett.* 22(1), 709–712 (2012).

37 Lu Y, Stinnette TW, Westrick E *et al.* Treatment of experimental adjuvant arthritis with a novel folate receptor-targeted folic acid-aminopterin conjugate. *Arthritis Res. Ther.* 13(2), (2011).

38 Matteson EL, Lowe VJ, Prendergast FG *et al.* Assessment of disease activity in rheumatoid arthritis using a novel folate targeted radiopharmaceutical Folatescan. *Clin. Exp. Rheumatol.* 27(2), 253–259 (2009).

39 Varghese B, Haase N, Low PS. Depletion of folate-receptor-positive macrophages leads to alleviation of symptoms and prolonged survival in two murine models of systemic lupus erythematosus. *Mol. Pharm.* 4(5), 679–685 (2007).

40 Jager NA, Westra J, Van Dam GM *et al.* Targeted folate receptor beta fluorescence imaging as a measure of inflammation to estimate vulnerability within human atherosclerotic carotid plaque. *J. Nucl. Med.* 53(8), 1222–1229 (2012).

41 Shen J, Chelvam V, Cresswell G, Low PS. Use of folate-conjugated imaging agents to target alternatively activated macrophages in a murine model of asthma. *Mol. Pharm.* 10(5), 1918–1927 (2013).

42 Jager NA, Westra J, Golestani R *et al.* Folate receptor-beta imaging using 99mTc-folate to explore distribution of polarized macrophage populations in human atherosclerotic plaque. *J. Nucl. Med.* 30(114), 143180 (2014).

43 Westendorp RG, Langermans JA, Huizinga TW *et al.* Genetic influence on cytokine production and fatal meningococcal disease. *Lancet* 349(9046), 170–173 (1997).

44 Gerstner ER, Duda DG, Di Tomaso E *et al.* VEGF inhibitors in the treatment of cerebral edema in patients with brain cancer. *Nat. Rev. Clin. Oncol.* 6(4), 229–236 (2009).

45 Kumar P, Shen Q, Pivetti CD, Lee ES, Wu MH, Yuan SY. Molecular mechanisms of endothelial hyperpermeability: implications in inflammation. *Expert. Rev. Mol. Med.* 30(11), e19 (2009).

46 Baluna R, Vitetta ES. Vascular leak syndrome: a side effect of immunotherapy. *Immunopharmacology* 37(2–3), 117–132 (1997).

47 Xia W, Low PS. Folate-Targeted Therapies for Cancer. *J. Med. Chem.* 53(19), 6811–6824 (2010).

48 A comparison of the number of publications on nanomedicines for the treatment of cancer versus autoimmune diseases. www.pubmed.org

49 Jain JP, Yenet Ayen W, Domb AJ, Kumar N. Biodegradable polymers in drug delivery. In: *Biodegradable Polymers in Clinical Use and Clinical Development.* Domb AJ, N Kumar, A Ezra (Eds). John Wiley & Sons Inc., NJ, USA, 1–58 (2011).